第33卷 第6期 焊 接 学 报 Vol. 33 No. 6
2012年6月 TRANSACTIONS OF THE CHINA WELDING INSTITUTION June 2012

钛合金超音频直流脉冲 GTAW 焊缝组织性能

杨明轩， 齐铂金， 从保强， 王乐笑
(北京航空航天大学 机械工程及自动化学院，北京 100191)

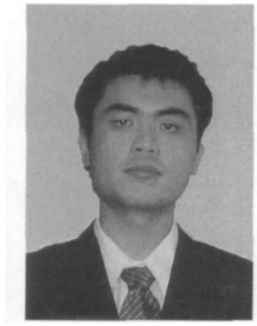
杨明轩

摘 要：基于1.5 mm厚Ti-6Al-4V(TC4)钛合金平板对接试验，研究分析了超音频直流脉冲氩弧焊焊缝金相组织及焊接接头力学性能. 结果表明，与常规直流钨极氩弧焊(gas tungsten arc welding，GTAW)相比，由于超音频直流脉冲方波电流的作用，气泡逸出速度增大，Ti-6Al-4V钛合金焊缝的气孔敏感性降低，熔池高温液态金属流动性增强，电弧能量集中，焊缝晶粒细化明显，其亚晶组织以短棒状α′马氏体组成的网篮状组织或α′片状组织与短棒状α′相交织的状态为主，焊接接头断后伸长率和断面收缩率显著提高.
关键词：超音频脉冲钨极氩弧焊；焊缝组织；力学性能；晶粒细化
中图分类号：TG403 文献标识码：A 文章编号：0253-360X(2012)06-0039-04

0 序 言

钛与钛合金具有较高的比刚度、优异的抗腐蚀性能，同时具有密度小，耐热性、韧性和焊接性好等特点，在航空航天、车辆工程、石油化工等各个领域应用广泛[1]. 目前使用的钛合金中有50%为α+β双相Ti-6Al-4V钛合金，针对其研究最为深入[2]. 由于钨极氩弧焊局部加热的工艺特点，常规直流GTAW钛合金焊件普遍存在接头晶粒粗大和组织不均匀的问题，因此控制焊接接头晶粒大小成为提高焊接结构质量的关键问题.

随着现代先进电源变换理论的发展，高频脉冲焊接作为一种先进的焊接工艺方法正在得到广泛应用和推广，研究表明在自由电弧的基础上加入高频脉冲电流可提高电弧稳定性，有利于改善和提高焊接质量[3]. 高频脉冲焊接时，周期性变化的电弧压力对熔池的搅拌作用能够破碎枝晶，增加熔池的结晶中心，促进焊缝晶粒细化，直接影响焊缝成形及接头力学性能. 国外学者研究发现，在Ti-6Al-4V钛合金GTAW焊接过程中，脉冲电流能细化晶粒[4,5].

文中基于Ti-6Al-4V钛合金进行了超音频直流脉冲GTAW平板对接试验，考查了该新型焊接技术对焊缝气孔敏感性、显微组织及接头力学性能的作用，对钛合金超音频直流脉冲GTAW焊缝组织及接头力学性能优化机理研究具有重要意义.

收稿日期：2011-04-25
基金项目：国家自然科学基金资助项目(50975015)

1 试验方法

采用1.5 mm厚的Ti-6Al-4V钛合金轧制平板，其化学成分如表1所示. 试样规格为170 mm×70 mm，焊前经酸洗去除氧化膜，用丙酮、无水乙醇擦拭. 电极为铈钨W-2%Ce，直径2.4 mm，弧长3 mm. 工艺参数如表2所示，沿轧制方向焊接，TC4焊丝直径1.6 mm，焊缝长度为160 mm，单面焊双面成形.

表1 Ti-6Al-4V钛合金化学成分(质量分数，%)
Table 1 Chemical compositions of Ti-6Al-4V plate material

Al	V	N	C	H	O	Fe	Ti
5.82	3.99	0.023	1.83	0.0007	0.063	<0.05	余量

截取焊缝按国家标准制备金相试样，腐蚀液为HF∶HNO_3∶H_2O=3∶10∶100；利用OLYPUMS BX51M型金相显微镜观察显微组织；利用2515X射线机检测缺陷；根据国家标准制备拉伸试样，如图1所示，每组参数做3个试件，利用万能试验机测试接头拉伸性能，

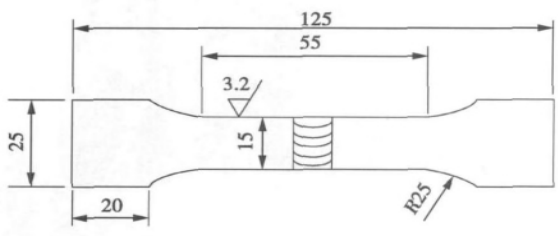

图1 拉伸试样(mm)
Fig. 1 Specimens of mechanical property test

表 2 Ti-6Al-4V 钛合金平板对接焊接工艺参数

Table 2 Parameters of welding process for Ti-6Al-4V titanium alloys

试样编号	基值电流 I_b/A	峰值电流 I_p/A	脉冲频率 f/kHz	占空比 δ(%)	电弧电压 U/V	保护气流量 q_c/(L·min^{-1}) 焊枪	焊缝背面	拖斗	焊接速度 v_1/(mm·min^{-1})	送丝速度 v_2/(mm·min^{-1})
1	118	—	—	—	10.2	15	20	3	210	260
2	60	140	20	50	9.0	15	20	3	210	260
3	80	160	40	50	9.5	15	20	3	270	320
4	75	155	40	50	9.3	15	20	3	240	290

每组测试结果为 3 个试样所得可信数据的平均值.

2 试验结果与讨论

2.1 焊缝气孔敏感性

在第 1 节所述的试验条件下获得表 2 中各组参数所对应的焊件，通过对比各组参数的 X 射线探伤发现，采用 1 号试样的焊接工艺参数所得焊件在焊趾处出现较大的独立散布气孔，在采用其它试样焊接工艺参数时几乎没有气孔，如图 2 所示.

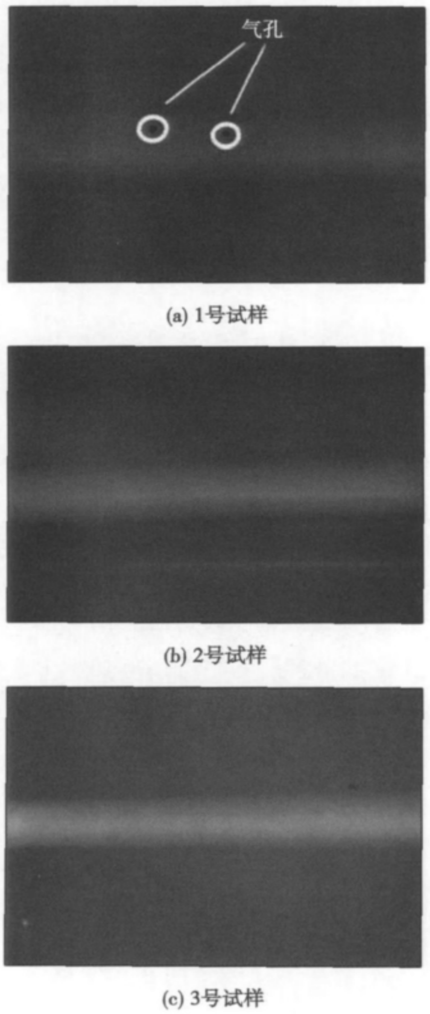

图 2 焊缝 X 射线探伤

Fig. 2 X-ray detection for welds

氢是钛及钛合金焊接形成气孔的主要原因，其在钛中的溶解度随温度升高而降低，熔池中部比熔池边缘温度高，故熔池中部的氢容易向熔池边缘扩散，故焊趾容易因为氢过饱和而生成气孔[6]，这也是图 2a 中焊趾处出现较大散布气孔的原因.

由文献[6]的论述可知，气孔的产生由气泡的生核、长大和上浮三个阶段组成，焊接熔池中存在大量现成表面，极易形成气泡核，气泡核形成后，在熔池金属中经过短暂的长大即向外逸出，逸出速度大于焊缝金属结晶速度则焊缝中不易形成气孔，故较大的气泡逸出速度将有利于减小焊缝中气孔形成的可能性. 气泡浮出速度为

$$v = \frac{2}{9}\frac{(\rho_1 - \rho_2) g r^2}{\eta} \tag{1}$$

式中：v 为气泡浮出速度；ρ_1 为液体金属的密度；ρ_2 为气体的密度；g 为重力加速度；r 为气泡的半径；η 为液体金属的粘度.

气泡长大需满足的条件如式(2)所示，由于焊接熔池内有许多现成表面，因此气泡多呈椭圆形，故可具有较大的曲率半径 R 以满足气泡长大的条件.

$$P_h > 1 + \frac{2\sigma}{R} \tag{2}$$

式中：p_h 为气泡内部压力；σ 为金属与气体间的表面张力.

气泡脱离现成表面的能力决定于液态金属、气相及现成表面间的表面张力，可由气泡与现成表面浸润角 θ 表征，较小的 θ 有利于气泡较快逸出，即

$$\cos\theta = \frac{\sigma_{1,g} - \sigma_{1,2}}{\sigma_{2,g}} \tag{3}$$

式中：θ 为气泡与现成表面的浸润角；$\sigma_{1,g}$ 为现成表面与气泡间的表面张力；$\sigma_{1,2}$ 为现成表面与熔池金属间的表面张力；$\sigma_{2,g}$ 为熔池金属与气泡间的表面张力.

分析认为，超音频直流脉冲方波电流产生径向脉动电磁收缩力，使得电弧产生收缩效应[7]，增强了电弧挺度，电弧压力有较大提高[8]，则熔池液态流体中压力增大. 对于附着于现成表面的气泡，一方面，熔池流体中增大的压力将沿现成表面的径向产生作用，对气泡形成挤压，曲率半径 r 增大，与现

成表面的接触面积增加，则由式(1)可知气泡的上浮速度增大，有利于气泡逸出，同时，根据液体压强物理规律，液态流体中压强处处相等，因此熔池中增大的压力将不影响悬浮于熔池中的气泡运动．另一方面，由于超音频直流脉冲 GTAW 电弧能量密度集中，与常规直流 GTAW 相比，熔池液态金属温度更高[9]，液体表面张力随温度的升高而降低，即 $\sigma_{1,2}$ 减小；如前文所述，气泡与现成表面的接触面积增加，即 $\sigma_{1,g}$ 增大；高频脉冲焊接产生较大的电磁搅拌力将增强熔池流动性[10]，即 $\sigma_{2,g}$ 增大．故由式(3)可知，上述表面张力的变化使浸润角 θ 减小，有利于气泡快速逸出，同时，熔池流动性的增强也将有利于悬浮于熔池中随流体流动的气泡逸出．另外电弧等离子流力对熔池表面的冲击增强了机械搅拌作用，可对胞状晶凹陷处的气泡起到连续冲击的作用，增强了气泡离开其表面的能力[11]，上述因素综合作用使得超音频直流脉冲 GTAW 的气孔敏感性降低．

2.2　焊缝金相组织

由第1节所述方法制备1～3号试样的焊缝金相试样，其焊缝宏观形貌和显微组织分别如图3和图4所示，其中1号试样为常规直流 GTAW 焊缝组织，2号和3号为超音频直流脉冲 GTAW 焊缝组织．1号试样焊缝熔合区宏观组织较为粗大，如图3a所示；2号和3号所得焊件晶粒细化效果明显，焊缝金相组织呈现等轴化趋势，如图3b，c所示．

1号试样焊缝熔合区针状 α′马氏体多为长条形，有少许网篮状组织出现，如图4a所示；3号试样熔合区晶粒尺寸显著减小，亚晶组织呈现以短棒状 α′马氏体组成的网篮状组织或 α′片状组织与短棒状 α′相交织为主的形态，如图4b所示．

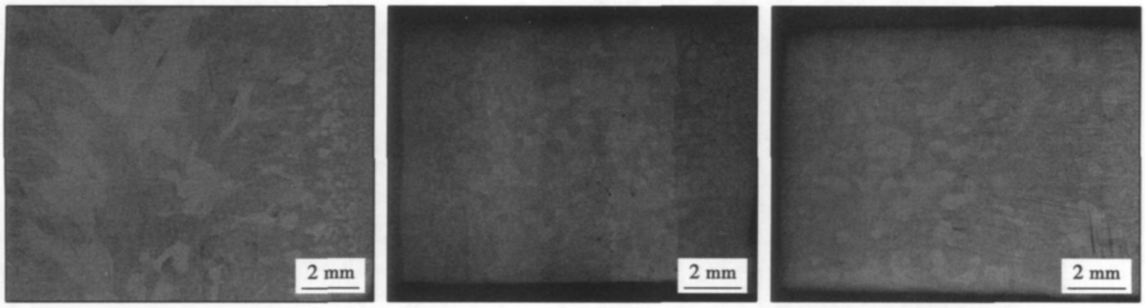

(a) 1号试样　(b) 2号试样　(c) 3号试样

图3　焊缝宏观组织
Fig. 3　Macrostructure of welds

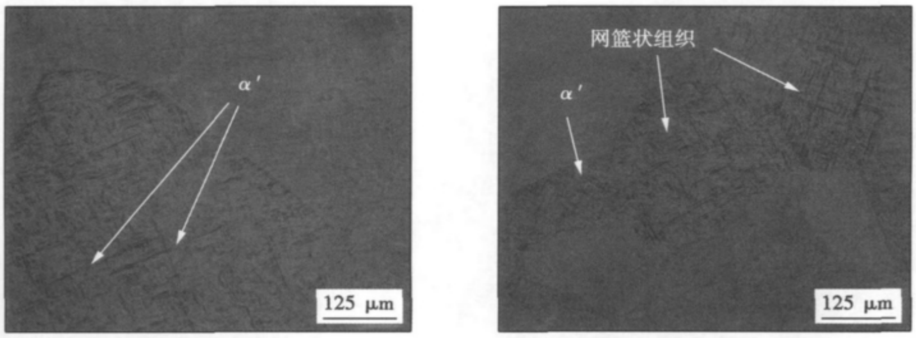

(a) 1号试样　(b) 3号试样

图4　焊缝中心区显微组织
Fig. 4　Microstructure of weld zone

分析认为，超音频脉冲 GTAW 电磁搅拌增强了熔池流动性，降低了焊缝中粗大柱状晶出现的可能，同时，高频脉冲焊接电弧能量密集，在焊件均焊透的前提下，其焊接热输入低于常规直流 GTAW，而热输入直接影响焊缝冷却速度及在 β 相变点以上的高温停留时间[12]，从而影响晶粒尺寸．随着热输入的减小，加热温度降低，高温停留时间缩短，冷却速度增大，β 相直接由体心立方晶格直接转变为密排六方过

饱和固溶体－α'六方马氏体[13,14]，而且$\beta \rightarrow \alpha'$过程形核率高，$\alpha'$丛尺寸变小，因此造成焊缝晶粒细化.

2.3　焊接接头力学性能

按照第1节所述试验方法，对表2中第1～3号试样及母材进行拉伸试验，其试验数据如表3所示. 与1号试样比较，2～4号试样焊后接头强度平均值几乎等同(均高于母材)，断后伸长率及断面收缩率平均值分别增长了35%和101%以上，同时考察试样断裂位置，1号试样在焊缝处断裂，2～4号试样断裂均在HAZ区，可知超音频直流脉冲GTAW焊缝强度提高.

表3　焊接接头力学性能

Table 3　Mechanical properties of welding joint

试样编号	抗拉强度 R_m/MPa	断后伸长率 A(%)	断面收缩率 Ψ(%)	断裂位置
0(母材)	1 052.80	12.54	—	—
1	1 117.10	5.85	10.05	焊缝
2	1 105.57	11.16	20.17	HAZ
3	1 110.63	11.44	23.93	HAZ
4	1 117.72	7.89	21.58	HAZ

如前所述，超音频直流脉冲GTAW电弧能量密集，过热面积小，较强的电磁搅拌效应大幅提升了熔池流动性，故冷却结晶后，焊缝中心区由短棒状α'马氏体组成的网篮状组织取代了常规直流GTAW的细长针状α'马氏体，晶粒细化显著，断后伸长率和断面收缩率增大，接头塑性增强.

3　结　论

(1) 与常规直流GTAW较大的气孔敏感性相比，超音频直流脉冲GTAW可有效消除焊缝气孔.

(2) 超音频直流脉冲GTAW接头组织晶粒细化明显，焊缝熔合区亚晶组织呈现短棒状α'马氏体组成的网篮状组织.

(3) 超音频直流脉冲GTAW焊接接头断后伸长率和断面收缩率显著提高.

参考文献:

[1] Leyens C, Peters M. Titanium and Titanium Alloys [M]. Germany: Wiley-VCH Verlag GmbH & Co. KGaA, Weinheim, 2003.

[2] 周水亮，陶　军，郭德伦. 细晶粒钛合金GTAW焊缝成形性能分析 [J]. 焊接学报, 2009, 30(7): 25－28.
Zhou Shuiliang, Tao Jun, Guo Delun. Appearance of fine grain titanium alloy by tungsten iner-gas arc welding (GATW) [J]. Transactions of the China Welding Institution, 2009, 30(7): 25－28.

[3] 从保强，齐铂金，周兴国. 超快变换高频变极性方波TIG电弧行为 [J]. 焊接学报, 2009, 30(6): 87－90.
Cong Baoqiang, Qi Bojin, Zhou Xingguo. TIG arc behavior of ultra fast-convert high-frequency variable polarity square wave [J]. Transactions of the China Welding Institution, 2009, 30(6): 87－90.

[4] Kishore B N, Ganesh S R S, Mythili R, *et al*. Correlation of microstructure with mechanical properties of TIG weldments of Ti-6Al-4V made with and without current pulsing [J]. Materials Characterization, 2007, 58(7): 581－587.

[5] Sundaresan S, Janaki D, Madhusudhan G. Microstructural refinement of weld fusion zones in α-β titanium alloys using pulsed current welding [J]. Materials Science and Engineering, 1999, 262(1/2): 88－100.

[6] 周振丰，张文钺. 焊接冶金与金属焊接性 [M]. 北京: 机械工业出版社, 1987.

[7] 赵家瑞，孙　栋，胡绳荪，等. 高频脉冲TIG焊电弧的阳极行为 [J]. 焊接学报, 1992, 13(1): 59－66.
Zhao Jiarui, Sun Dong, Hu Shengsun, *et al*. Arc behavior of high frequency pulse TIG welding arc [J]. Transactions of the China Welding Institute, 1992, 13(1): 59－66.

[8] Onuki J, Yoshisa A, Masayasu N, *et al*. Development of a new high-frequency, high-peak current power source for high constricted arc formation [J]. Journal of Applied Physics, 2002, 41(9): 5821－5826.

[9] 李　薇. A-TIG焊工艺及深熔机理研究 [D]. 北京: 北京航空航天大学, 2006.

[10] Atthey D R. A mathematical model for fluid flow in a weld pool at high currents [J]. Journal of Fluid Mechanics, 1980, 98(4): 787－801.

[11] 许海鹰. 超音频直流脉冲TIG焊技术及工艺适用性研究 [D]. 北京: 北京航空航天大学, 2009.

[12] 吴　巍，高洪明，吴　林. 细晶粒钛合金粗晶区组织及接头力学性能分析 [J]. 焊接学报, 2008, 29(1): 61－64.
Wu Wei, Gao Hongming, Wu Lin. Microstructures in CGHAZ and mechanical properties of welded joint during welding of fine grain titanium alloy [J]. Transactions of the China Welding Institution. 2008, 29(1): 61－64.

[13] Ahmed T, Rack H J. Phase transformation during cooling ina＋b titanium alloys [J]. Materials Science & Engineering, 1998, A243(3): 206－211.

[14] Elmer J W, Palmer T A. Phase transformation dynamics during welding of Ti-6Al-4V [J]. Journal of Applied Physics, 2004, 95(12): 8327－8339.

作者简介: 杨明轩，男，1985年出生，博士研究生. 主要从事高频脉冲氩弧焊电弧及接头组织性能研究. Email: oybenq@gmail.com

通讯作者: 齐铂金，男，教授. Email: qbj@buaa.edu.cn

Abstract: Based on explicit analysis, a 3D FE model coupled with thermo-mechanical of radial friction lap welding joint was established with 45 steel by applying ABAQUS software. Assuming that the deformation rate is known, it is discussed the field of temperature on the welding interface and the loading force on the radial ring in the paper. Using the Johnson-cook constitutive model, thermal properties, friction coefficient changing with temperature and plastic deformation heat were also considered, The temperature field distribution and the deviation of loading pressure were predicted and analyzed. The results show that without considering the heat transfer of the radial ring and the fixture, the radial ring is formed to fixture as the center to form an elliptical temperature gradient distribution and to fixture void as the center to form an strip temperature gradient distribution. The maximum temperature reached 1 260 ℃ and 1 050 ℃. In order to simplify the welding process, the loading force curve fit for three compression process. The explicit analysis, the standards and the constitutive model were feasible.

Key words: radial friction welding; temperature field; friction heat; numerical simulation

Microstructure and properties of titanium alloys welds using ultrasonic frequency pulse GTAW YANG Mingxuan, QI Bojin, CONG Baoqiang, WANG Lexiao (School of Mechanical Engineering and Automation, Beihang University, Beijing 100191, China). pp 39 – 42

Abstract: Based on butt welding during Ti-6Al-4V (TC4) titanium alloys plate with the thickness of 1.5mm, microstructure of weld face and properties of welded joint were investigated by ultrasonic frequency pulse gas tungsten arc welding (GTAW). Compared with conventional direct current GTAW process, the experimental results show that ultrasonic frequency pulse current causes the energy concentration with an obvious pinch effect of arc plasma and the increasing escape speed of gas pore. Grain refining and the elimination of gas pore are due to the enhancement of fluid flow by ultrasonic frequency pulse GTAW process for Ti-6Al-4V titanium alloys. The main structure of subcrystal is the basketweave microstructure composed of rod-shaped martensite or the interlaced microstructure composed of both rod-shaped and plate phase. Similarly, ultrasonic frequency pulse GTAW process could also improve the elongation and reduction of area.

Key words: ultrasonic frequency pulse GTAW process; microstructure; mechanical properties; grain refining

Effect of holding time on interface structure and bonding strength of diffusion bonding joint of TiAl and Ni-based alloy LI Haixin, LIN Tiesong, HE Peng, WEI Hongmei, FENG Jicai (State Key Laboratory of Advanced Welding and Joining, Harbin Institute of Technology, Harbin 150001, China). pp 43 – 46

Abstract: Diffusion bonding of TiAl to Ni-based alloy (GH99) with Ti interlayer was carried out. The reaction products and the interface structures of the joints were investigated by scanning electron microscopy, electron probe X-ray microanalysis and X-ray diffraction. The results show that four kinds of reaction layers are formed at the interface between the GH99 alloy and Ti interlayer, such as $(Ni,Cr)_{ss}$, rich Ti-$(Ni,Cr)_{ss}$, TiNi and Ti_2Ni. When the holding time is short, $Ti(Al)_{ss}$ layer is formed at the interface between Ti interlayer and TiAl alloy. With the holding time increasing, the $Ti(Al)_{ss}$ reaction layer transformed into Ti3Al and Al_3NiTi_2. With the holding time increasing, the thickness of TiNi reaction layer increases, while the thickness of Ti_2Ni layer increases firstly and then decreases. The shear test results show that the shear strength of the joint increases at first, then decreases, and then increases with the holding time increasing. The fractographs of the joints show that the fracture mainly occurs in the Ti_2Ni reaction layer.

Key words: titanium aluminium alloy; Ni-based alloy; diffusion bonding; interface structure; shear strength

Relationship between metal transfer and arc shape in twin-wire indirect arc welding CAO Meiqing[1], ZOU Zengda[2], QU Shiyao[2] (1. College of Material Science and Engineering, SUST, Qingdao, Shandong 266510, China; 2. College of Material Science and Engineering, Shandong University, Jinan 250061, China). pp 47 – 50

Abstract: Relationship between metal transfer, arc shape and arc voltage was investigated with high speed camcorder system and digital oscillograph. Results show that metal transfer has a close relationship with arc voltage and the regular variation of arc shape. It shows that the regular changes of metal transfer make polarity spots spacing and arc beam resistance change and cause the arc voltage fluctuations, so that the arc shape changes regularly. Droplet transfer pattern changes and droplet size dereases with the increasing of welding current, different metal transfer mode has different arc voltage fluctuation, spraying transfer has lower variation of voltage but short transfer's arc voltage variation is bigger.

Key words: metal transfer; arc shape; arc voltage

Study on process and property of FSW of spray formed 7055 aluminum alloy YAN Keng, LIU Jun, SHI Chao (Provincial Key Lab of Advanced Welding Technology, Jiangsu University of Science and Technology, Zhenjiang 212003, China). pp 51 – 54

Abstract: Friction-stir welding was employed in the welding experiment of spray formed 7055 aluminium alloy plate with thickness of 4 mm. The influence of the rotating rate and the welding speed on the mechanical properties of the joint, microstructure of the weld, and the fracture mode were analyzed. The results showed that good-looking, defectless welds could be obtained with proper welding parameters. The mechanical properties of the joints were related to the welding parameters. When the rotating rate was 1 000 r/min and the welding speed was 100 mm/min, the joints achieved good mechanical properties. The tension strengths of the joints reached 455 MP, and the fracture mode was ductile and brittle mixed. The welds consisted of three zones, among which the weld-nugget zone consisted of fine equiaxed grains. The minimum micro-hardness occurred on the advancing side, which indicated the advancing side is the weakness of the weld.

Key words: spray formed 7055 aluminium alloy; FSW; welding process; microstructure